3D Methods for Examining Soil–Building Interaction for Nonlinear Soil Behavior Based on an Input Wave Field

Masahiro Iida, A.M.ASCE[1]

Abstract: This paper proposes three-dimensional (3D) simplified nonlinear methods for examining the soil–building interaction for nonlinear behavior of soils based on an input seismic wave field. A seismic wave field is defined as seismic waves propagating in a 3D medium. The proposed 3D methods were developed on the basis of the 3D linear method, which was recently proposed to adequately treat seismic surface waves trapped by a several-kilometer-deep underground structure. To demonstrate the feasibility of the proposed methods, interaction analyses of a midrise RC building and a wood building were performed in the reclaimed zone of Tokyo Bay in the cases of soils with linear, nonlinear, and liquefaction behavior for the 1923 Kanto earthquake. These interaction analyses provide a reasonable evaluation of building performance. In particular, building responses became excessively large, following extremely large increases in the amplitudes of surface waves in liquefied soils. The building responses provide significant clues for interpreting a typical damage pattern in which Japanese RC building damage is concentrated on the first story. **DOI: 10.1061/(ASCE)GM.1943-5622.0000780.**

Author keywords: Structural dynamics; Three-dimensional analysis; Nonlinear analysis; Soil liquefaction; Soft soils; Soil–structure interactions; Surface waves; Underground structure.

Introduction

A soil–building interaction analysis is of great benefit for estimating the seismic dynamic responses of various buildings. In addition to soil–building interaction effects, an interaction analysis includes consideration of all vibration modes, composed of building modes and soil modes. In an interaction analysis, the treatment of seismic external force seems to be the most important issue to be resolved. Actually, a considerable amount of short-period (less than a few seconds) surface waves were often detected in ground motions observed at a soft-soil site (Johnson and Silva 1981; Kinoshita et al. 1992). Although the predominant periods of S waves and surface waves are almost identical, the vertical amplitude distributions of these waves can be very different in surface layers at a soft-soil site (Iida and Kawase 2004; Iida et al. 2005). Therefore, it is necessary to identify S waves and surface waves and to treat them separately in a soil–building interaction analysis.

However, an inherent feature of surface waves brings great difficulty in handling surface waves in a soil–building interaction system. The vertical increase in the amplitudes of short-period surface waves in a shallow (several tens of meters) underground structure depends largely on the material properties of the deep (several kilometers) underground structure in which surface waves propagate. This inherent feature of surface waves, which was explained mathematically in a soil response study (Iida 2006), means that surface-wave incidence into a shallow soil model is not valid for surface waves trapped by a deep structure.

Moreover, to accomplish a realistic soil–building interaction analysis, material nonlinearity of the soil and the building must be handled properly. At a soft-soil site, the vertical increase in the amplitudes of surface waves is much greater than that in S waves in soft sediment (Iida and Kawase 2004; Iida et al. 2005), so surface waves should contribute more to nonlinear behavior of the soil and the building. For the last three decades, a variety of nonlinear soil–structure interaction analyses have been performed (Bielak and Christiano 1984; Kim and Roesset 2004). Recently, an increasing number of soil–structure interaction analyses due to liquefaction were conducted (Koutsourelakis et al. 2002; Maheshwari and Sarkar 2011). However, almost no analyses have taken surface waves into account in a reasonable manner.

In this context, to treat short-period seismic surface waves adequately in a soil–building interaction analysis, Iida (2013) proposed a three-dimensional (3D) linear FEM for examining soil–building interaction based on an input seismic wave field. An input seismic wave field means that forces produced by body and surface waves propagating in the 3D soil volume of a soil–building interaction system are employed as external forces in the finite-element (FE) calculations, which will be described mathematically in the next section of this paper. To confirm the validity of the method, linear responses of low- to high-rise RC model buildings were calculated for a hypothetical large earthquake in the lakebed zone of Mexico City.

A subsequent study (Iida et al. 2015) confirmed the validity of the proposed method. After some improvements in the method were made, it was applied to calculate seismic responses of a midrise RC building and a wood building for the 1923 Kanto earthquake (earthquake magnitude determined by the Japanese Meteorological Agency as M_J = 8.1) in the reclaimed zone of Tokyo Bay. The building responses also were compared with those calculated by two standard approaches, and it turned out that the proposed method was able to estimate building responses more accurately.

On the other hand, in advance of the two previously mentioned soil–building interaction studies (Iida 2013; Iida et al. 2015), 3D simplified nonlinear FE soil response methods based on an

[1]Earthquake Research Institute, Univ. of Tokyo, 1-1-1, Yayoi, Bunkyo-ku, Tokyo 113-0032, Japan. E-mail: iida@eri.u-tokyo.ac.jp

Note. This manuscript was submitted on January 11, 2016; approved on June 30, 2016; published online on August 25, 2016. Discussion period open until January 25, 2017; separate discussions must be submitted for individual papers. This paper is part of the ***International Journal of Geomechanics***, © ASCE, ISSN 1532-3641.

input seismic wave field were proposed in the previously mentioned soil response study (Iida 2006). In this study, 3D linear, nonlinear, and liquefaction soil response analyses were performed. Combining the nonlinear soil response methods with the linear method for soil–building interaction (Iida et al. 2015), the present study proposes 3D simplified FE methods for examining the soil–building interaction for nonlinear behavior of soils based on an input seismic wave field. In the proposed methods, the nonlinear soil formulations are incorporated into the linear method for soil–building interaction.

The present study is aimed at demonstrating the feasibility of the proposed methods in which an input wave field is modified according to varied soil properties predicted by the methods. As an application, interaction analyses of a midrise RC building and a wood building were performed in the reclaimed zone of Tokyo Bay in the cases of soils with linear, nonlinear, and liquefaction behavior for the 1923 Kanto earthquake. This study attempted to not underestimate the building responses, predicting that they will be overestimated by the linear building behavior.

In the following three sections, the methods are presented in the cases of soils with linear, nonlinear, and liquefaction behavior. Next, a soil response study (Iida 2006) is reviewed in which linear, nonlinear, and liquefaction soil response analyses were performed in the reclaimed zone of Tokyo Bay for the 1923 Kanto earthquake. Please note that the earthquake-area pair studied by Iida (2006) is used in the present study. Finally, soil–building interaction analyses are performed in the cases of soils with the three types of behaviors. As two representative model buildings, a midrise RC building with piles and a wood building without piles are used. The two buildings are identical to those used by Iida et al. (2015), in which only linear soil–building interaction analyses were conducted for the same earthquake-area pair as the present study.

Linear Method

This section outlines the 3D linear FE method for examining soil–building interaction based on an input seismic wave field. The linear method was proposed in a recent study (Iida 2013), and was improved in a subsequent study (Iida et al. 2015). In the following paragraphs, only the fundamentals of the method are described. Fig. 1 illustrates the 3D superstructure–foundation–pile–soil systems used, which were the same as those used in the two studies. The interaction systems were developed originally in a work by Ishihara and Miura (1993).

The lumped-mass stick-building superstructure rested on a rigid box foundation supported on piles. The superstructure was modeled as a shear spring system, and sway and rocking of the foundation were considered. The horizontal degree of freedom of each story was coupled with the rocking degree of freedom at the foundation. Each pile was modeled by beam elements, and the soil volume was modeled by 3D rectangular prism elements. To allow the relative movement (slip) of the pile with respect to the soil, joint spring elements were attached to both edges of each beam element that formed the pile. In this way, the interaction between the pile and the soil was considered. The side and bottom boundaries of the soil volume were equipped with viscous dampers.

The equation of motion that connects the superstructure, the foundation, the piles, and the soil is represented by the following formulation:

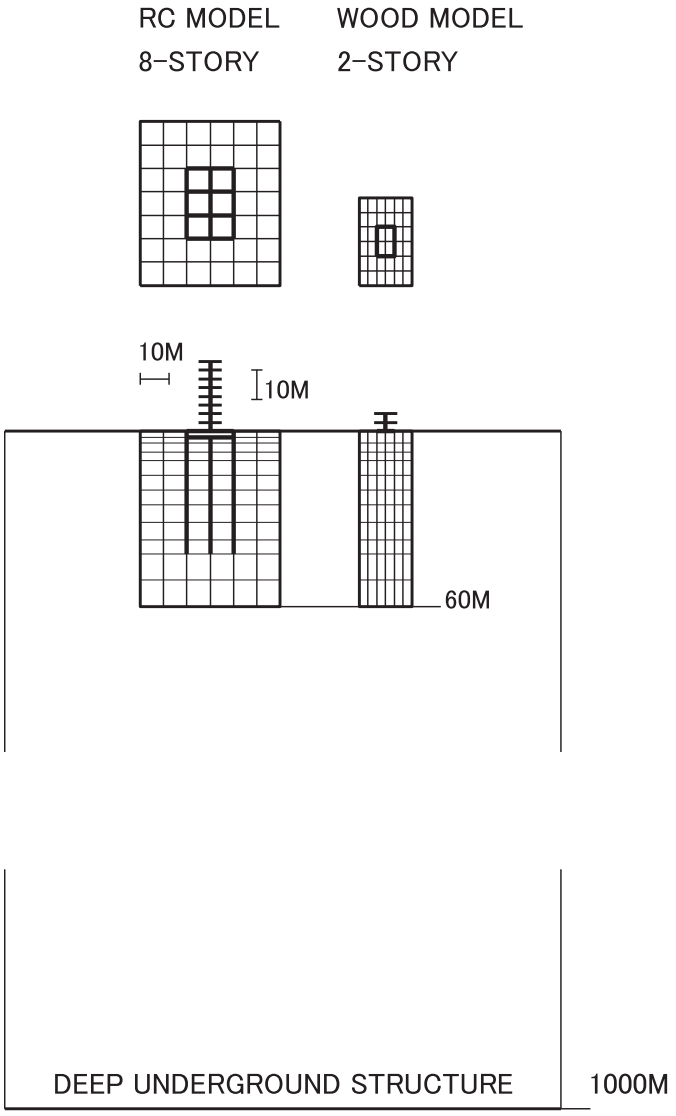

Fig. 1. Plan sections and cross sections (north–south direction) of 3D superstructure–foundation–pile–soil systems for the two buildings; one-dimensional appropriate deep underground structure used to estimate input wave field is also displayed

$$[M]\left\{\delta^2\chi_a/\delta t^2\delta^2\chi_b/\delta t^2\delta^2\chi_c/\delta t^2\delta^2\chi_d/\delta t^2\delta^2\chi_e/\delta t^2\right\}^T + [C]\left\{\delta\chi_a/\delta t\delta\chi_b/\delta t\delta\chi_c/\delta t\delta\chi_d/\delta t\delta\chi_e/\delta t\right\}^T + [K]\left\{\chi_a\chi_b\chi_c\chi_d\chi_e\right\}^T = \left\{F_aF_bF_cF_dF_e\right\}^T \quad (1)$$

where $[M]$ = mass matrix; $[C]$ = damping matrix; $[K]$ = stiffness matrix; $\{\chi\}$ = displacement vector associated with the system; $\{F\}$ = external force vector; and t = time. The superscript T denotes the transposed vector, and subscripts a, b, c, d, and e correspond to the superstructure, the foundation, the piles or the soil body, the side boundaries of the system, and the bottom boundary of the system, respectively. The linear equation of motion is solved by the Newton-Raphson technique.

The multilayered soil volume of the 3D (x, y, z) soil–building interaction system is subject to horizontal ground motions. As an input wave field, vertically propagating plane S waves and horizontally propagating plane surface waves are imposed upon the soil volume of the 3D system. Then, the external force vector is expressed by

$$\{F_aF_bF_cF_dF_e\}^T = [M]\{0\ \delta^2 p_b/\delta t^2 + \delta^2 q_b/\delta t^2\ \delta^2 p_c(z)/\delta t^2 + \delta^2 q_c(x,y,z)/\delta t^2\ \delta^2 p_d(z)/\delta t^2 + \delta^2 q_d(x,y,z)/\delta t^2\ \delta^2 p_e/\delta t^2 + \delta^2 q_e(x,y)/\delta t^2\}^T \quad (2)$$

where p and q = external displacements contributed by S waves and surface waves in the soil volume of the system, respectively. The p and q terms are computed on the basis of Eqs. (1)–(4) in a soil response study (Iida 2006). An S-wave field and a surface-wave field are separately estimated in the soil volume by applying elastic wave theory to an appropriate deep underground structure (Fig. 1), after surface ground motions are separated into S waves and surface waves. The whole-wave field used as input is the summation of the two wave fields.

Method for Nonlinear Behavior of Soils

This section describes the 3D simplified method for examining the soil–building interaction for nonlinear behavior of soils based on an input seismic wave field. In the new method, existing nonlinear soil formulations are incorporated into the previously mentioned linear method (Iida et al. 2015). Therefore, only the fundamentals are described here. The nonlinear equation of motion is expressed by Eq. (1), and is solved by the Newton-Raphson technique. The method assumes nonliquefiable soils, and employs the nonlinear soil formulations that were described in a soil response study (Iida 2006).

This method adopts a bilinear model of soils with a 3D Mohr-Coulomb failure criterion. The four kinds of nonlinear parameters used in the bilinear model are the cohesion, the frictional angle, the second rigidity, and the damping coefficient of each shallow layer that might behave in a nonlinear fashion. The mathematical formulations and the nonlinear techniques of the bilinear model were provided fully in a previous soil response study (Iida 1999), in which only S-wave portions were treated, and an input base motion was employed.

The external force vector is expressed by Eq. (2). An S-wave field and a surface-wave field are separately estimated for soils with nonlinear behavior in the soil volume of the 3D soil–building interaction system, by applying elastic wave theory to an appropriate deep underground structure (Fig. 1) varied by the nonlinear behavior, on the basis of the linear wave fields constructed for elastic soils. The wave fields are called *nonlinearly modified wave fields*. The modified whole-wave field used as input is the summation of the two modified wave fields. Practically, in accordance with the bilinear model of soils, a simplified two-stage modified wave field is assumed, which is composed of the initial wave field for elastic soils and the varied wave field for soils with nonlinear behavior.

The varied S- and surface-wave fields are expressed by the following equation. Here, it is assumed that ground motions observed at a sufficient depth relative to surface layers are not influenced by nonlinear behavior of soils anticipated in the surface layers

$$FSar^{\mathrm{NON}} = FSRar/de^{\mathrm{NON}}FSde^{\mathrm{NON}} = FSRar/de^{\mathrm{NON}}FSde = FSRar/de^{\mathrm{NON}}FSsu/FSRsu/de \quad (3)$$

where FSd is the Fourier spectrum of a seismogram at a depth of d, and $FSRd1/d2$ is the Fourier spectral ratio between two seismograms at depths of $d1$ and $d2$. A superscript NON indicates a soil with nonlinear behavior, and the subscripts ar, su, and de denote an arbitrary depth, the ground surface, and a sufficient depth relative to surface layers, respectively.

Method for Liquefaction Behavior of Soils

This section explains the 3D simplified method for examining the soil–building interaction for liquefaction behavior of soils based on an input seismic wave field. In the new method, existing liquefaction soil formulations are incorporated into the previously mentioned linear method (Iida et al. 2015). Therefore, only the fundamentals are described here. The liquefaction equation of motion is expressed by Eq. (1), and is solved for time-variable soil materials by the Newton-Raphson technique. The method assumes that nonliquefiable soils behave in a linear manner, and employs the liquefaction soil formulations that were described in a soil response study (Iida 2006).

The method adopts a simple liquefaction model of soils that considers neither pore-water pressure buildup nor vertical water flow. As the main features of the model, it is assumed that a full liquefaction process gets completed for a short time at a liquefied soil element, if the shear strain at the soil element reaches a given criterion value in any of two horizontal directions. Also, during the liquefaction process at the soil element, four soil material parameters (P-wave velocity, S-wave velocity, density, and damping coefficient) change at a constant speed. Thus, the six kinds of liquefaction parameters used in the liquefaction model are the criterion shear strain and the process time at the liquefied soil element, and the four soil material parameters of fully liquefied soils. Although the soil materials are time variable during a full liquefaction process, a linear solution scheme is available at each time step.

The external force vector is expressed by Eq. (2). An S-wave field and a surface-wave field are separately estimated for soils with liquefaction behavior in the soil volume of the 3D soil–building interaction system, by applying elastic wave theory to an appropriate deep underground structure (Fig. 1) varied by the liquefaction behavior, on the basis of the linear wave fields constructed for elastic soils. The wave fields are called "liquefaction-modified wave fields." The modified whole-wave field used as input is the summation of the two modified wave fields. Practically, following the simple liquefaction model of soils, a simplified two-stage modified wave field is assumed, which is composed of the initial wave field for elastic soils and the varied wave field for soils with liquefaction behavior.

The varied S- and surface-wave fields are expressed by the following equation. Here, it is assumed that ground motions observed at a sufficient depth relative to surface layers are not influenced by liquefaction behavior of soils anticipated in the surface layers

$$FSar^{\mathrm{LIQ}} = FSRar/de^{\mathrm{LIQ}}FSde^{\mathrm{LIQ}} = FSRar/de^{\mathrm{LIQ}}FSde = FSRar/de^{\mathrm{LIQ}}FSsu/FSRsu/de \quad (4)$$

where the superscript LIQ indicates a soil with liquefaction behavior.

Soil Responses

This section reviews some significant results that were obtained in a soil response study (Iida 2006), in which response analyses of soils

with linear, nonlinear, and liquefaction behavior were carried out on the basis of input wave fields. In the soil response study, free-field soil responses were computed for the 1923 Kanto earthquake at the Echujima borehole station located in the reclaimed zone of Tokyo Bay (Fig. 2). This earthquake-station pair is employed in the present study. Table 1 shows the deep multilayered structural model used at the Echujima station, which is characterized by a topmost 40 m of soft silty sediment.

In the soil response study, using the deep structural model, input wave fields were estimated. At the Echujima station, surface waves (Love waves), which had larger increase in the amplitudes than S waves in the soft sediment, were more dominant than at another (the Toyo) borehole station located in the reclaimed zone (Iida et al. 2005). This result was further reinforced by theoretical calculations for surface waves (Rayleigh waves) performed in the reclaimed zone of Tokyo Bay (Iida and Hatayama 2007). For this reason, the Echujima station was selected in the soil response study, and was again selected in the present study.

First, in the linear soil response analysis of the soil response study, a wave field was reproduced well as the simulated soil responses based on the wave field used as input. Fig. 3 displays the linearly simulated soil responses based on the input wave field estimated at the Echujima station for the Kanto earthquake. Throughout the present study, the two horizontal components were treated, and only the north–south components are displayed. The two depths of 6 and 19 m were in the soft sediment, and the 6-m depth laid in liquefiable layers that will be explained in the last paragraph of this section. The depth of 38 m corresponds to a depth of the sediment and bedrock interface (Table 1). The wave trains were largely amplified around the predominant period of the ground of approximately 1.0 s.

Second, in the nonlinear soil response analysis in which the nonlinear parameters of Table 2 were used, the nonlinearly modified input wave field was replaced by the original linear input wave field for a few reasons, and it was found that soils acted in a nonlinear fashion in the soft layers above 25 m in depth. Fig. 4 exhibits the nonlinearly simulated soil responses based on the input wave field. The amplitudes of the nonlinearly simulated time histories are slightly smaller compared with the amplitudes of the linearly simulated ones (Fig. 3), whereas the vibration period of the ground is much the same as the predominant period of the ground.

Table 1. Deep Multilayered Structural Model Used at the Echujima Borehole Station

Depth (m)	P-wave velocity (m/s)	S-wave velocity (m/s)	Density (t/m^3)	Damping coefficient
0–4	620	110	1.70	0.045
4–10	940	110	1.70	0.045
10–16	1,330	130	1.60	0.038
16–26	1,330	130	1.70	0.038
26–34	1,330	230	1.70	0.022
34–38	930	230	1.70	0.022
38–53	1,750	440	2.00	0.011
53–70	1,750	440	1.85	0.011
70–75	1,750	300	1.85	0.017
75–83	1,750	460	1.85	0.011
83–100	1,750	460	1.90	0.011
100–210	1,830	500	1.90	0.010
210–1,000	1,830	880	1.90	0.006
1,000–	1,830	880	1.90	0.006

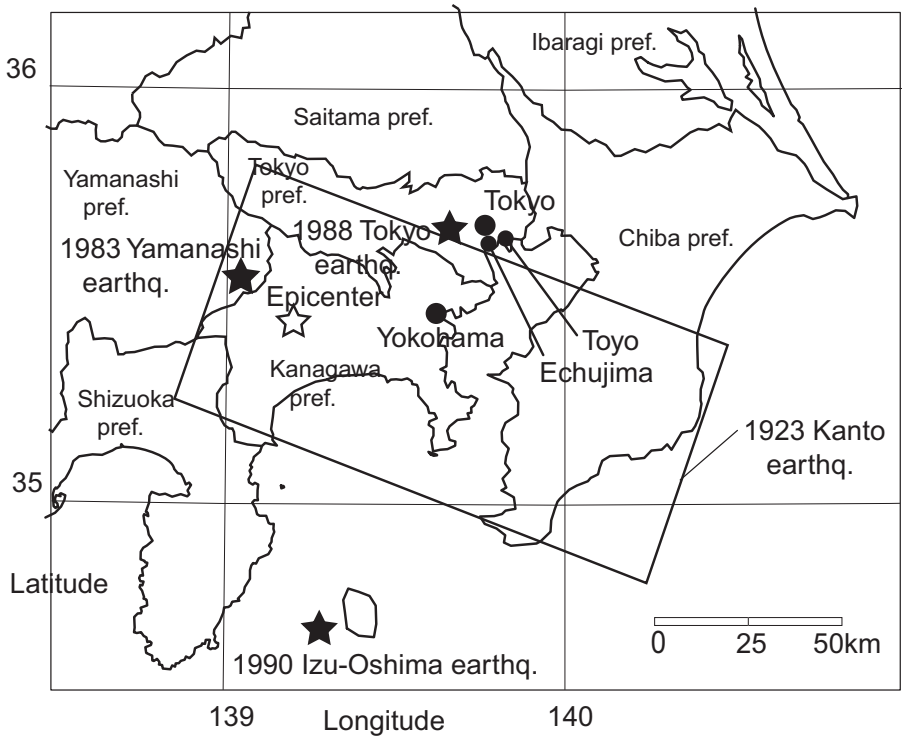

Fig. 2. Location map of Kanto region of Japan with projected surface fault geometry of 1923 Kanto earthquake and epicenter indicated by an open star [Note: Filled stars mark the epicenters of three medium-sized earthquakes; accelerograms recorded during medium-sized events were used to estimate wave fields for the Kanto earthquake; small filled circles mark Echujima and Toyo borehole stations (reprinted from Iida et al. 2015, © ASCE)]

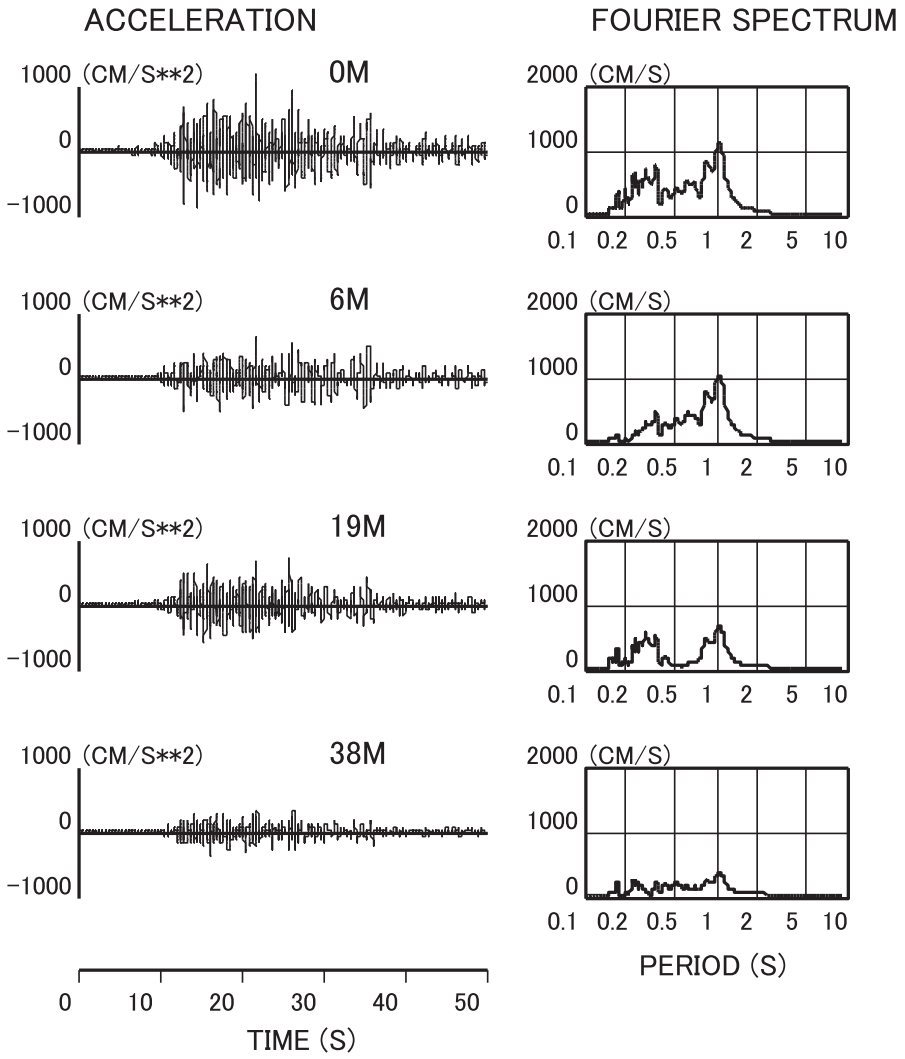

Fig. 3. FE linearly simulated soil responses at four depths based on input wave field estimated at Echujima station for the 1923 Kanto earthquake

Table 2. Nonlinear and Liquefaction Behavior of Soils Assumed in Surface Layers and Two Nonlinear Parameters of Soils

Depth (m)	Material	Nonlinear behavior	Liquefaction behavior	Cohesion (kN/m^2)	Frictional angle (°)
0–10	Silt	Possible	Possible	30.4	0
10–25	Clay and silt	Possible	—	54.9	0
25–38	Silt	Possible	—	147.0	0
38–60	Sand	—	—	—	—

Third, in the liquefaction soil response analysis, only the surface layers above 10 m were supposed to have liquefaction potential (Table 2). In the practical analysis, as soon as the main motions of long duration started, soils became fully liquefied in a depth range of 2–10 m. Whereas S waves were not much affected by liquefaction, the amplitudes of surface waves were increased excessively at the predominant period of the ground. Fig. 5 plots the liquefaction-simulated soil responses based on the "liquefaction-modified" input wave field. Indeed, the liquefaction-simulated traces were much larger than the linearly simulated traces (Fig. 3) in the surface layers above 10 m, although the vibration period of the ground changed little due to liquefaction.

Building Responses

In this section, interaction analyses of an 8-story RC model building and a 2-story wood model building are performed in the cases of soils with linear, nonlinear, and liquefaction behavior at the Echujima station for the 1923 Kanto earthquake. The two earthquake-station-and-building combinations were the same as those employed in a recent study (Iida et al. 2015), in which linear soil–building interaction analyses were performed, and the two buildings resonated severely with ground motions.

Fig. 1 illustrates the soil–building interaction systems for the 8-story RC (left) and the 2-story wood (right) buildings. Typical model buildings based on Japanese building codes were employed (Building Center of Japan 2013). Parameters used for the superstructures and the foundations of the two buildings are summarized in Table 3, and parameters used for the piles of the RC building are listed in Table 4. Please note the very high stiffness of the RC building and the very low stiffness of the wood building. The horizontal stiffness and the vertical stiffness of the joint spring element that connects a node for the pile and another node for the soil were exactly the same as those used in the previously mentioned recent study (Iida et al. 2015). In the case of the wood building, the foundation without piles was fixed to the soil. Also, because of computational difficulty, the

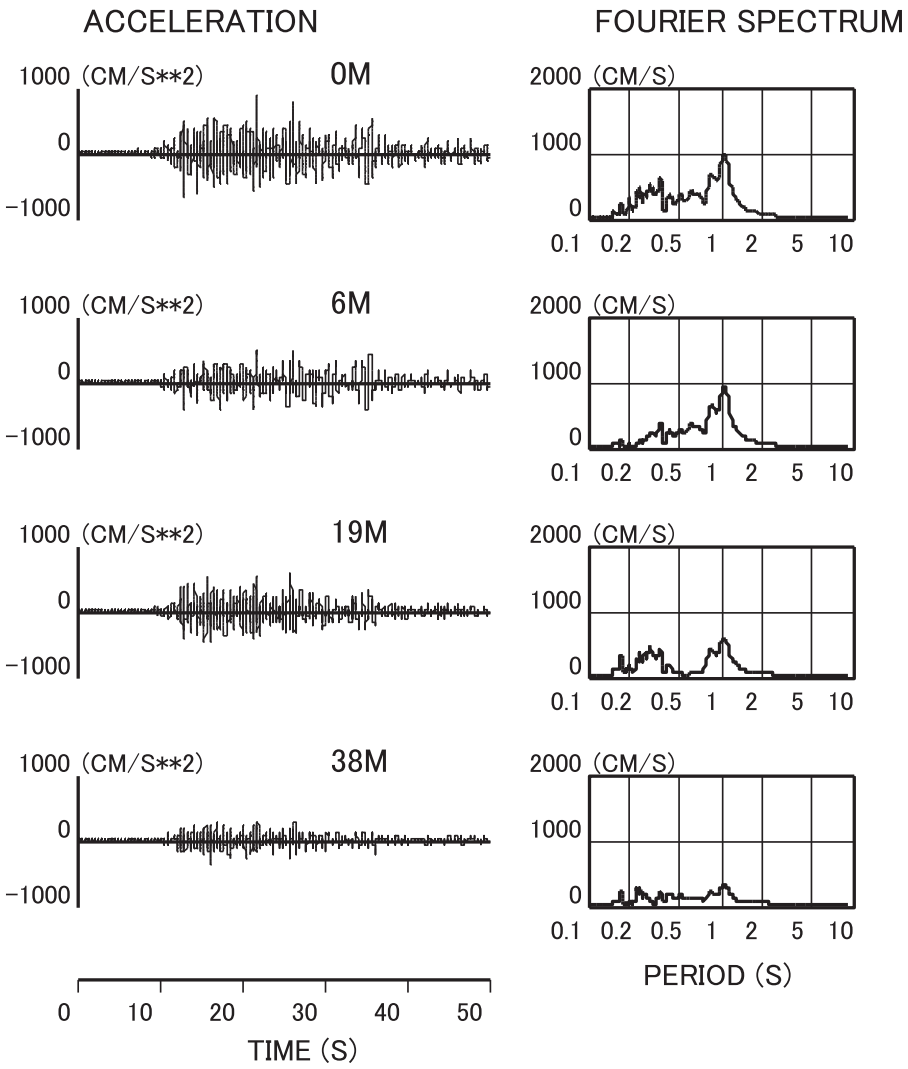

Fig. 4. FE nonlinearly simulated soil responses at four depths based on input wave field estimated at Echujima station for the 1923 Kanto earthquake

thin (0.5-m) embedment of the foundation was not considered, and a foundation model without the embedment was adopted.

Throughout the present study, the soil–building analyses were performed for 50 s with a time interval of 0.01 s. The effective period range was greater than approximately 0.2 s. In the linear analysis, a damping coefficient h of 0.05 was assigned for the two buildings. In the analyses for nonlinear and liquefaction behavior of soils, a larger damping coefficient h of 0.10 was assigned for the two buildings because larger damping is suitable for the inelastic analyses.

The maximum response values of the superstructures of the two buildings calculated by the three types of analyses are compared in Table 5. The very large building responses were presumably caused by the linear building behavior, and the absolute values do not make sense. In the nonlinear analysis of soils, the building responses were smaller than those calculated by the linear analysis, because of the larger building damping and the soil damping expressed by the shear stress–strain hysteresis curve. In the liquefaction analysis of soils, full liquefaction occurred at between 2 and 10 m of depth, and it produced excessively large building responses. However, caution might be required about the building responses obtained by the extreme assumption of full liquefaction, because partial liquefaction seems to be realistic.

To inspect the behavior of the two buildings in detail, the vertical distributions of the maximum interstory drift and the maximum shear force of the superstructures of the two buildings were compared among the three kinds of soils. The vertical distributions of the RC building are displayed in Fig. 6. The nonlinear behavior of the soil rendered the interstory drift somewhat small and the shear force considerably small. In the liquefaction analysis of soils, remarkably, the first story suffered particularly large interstory drift and shear force. The building performance can be interpreted as follows.

In the Soil Responses section of this paper, the liquefied soil responses were outstandingly large in the surface layers above 10 m (Fig. 5). Accordingly, the foundation and the piles of the RC building should suffer excessively large shear force in only the surface layers. On the other hand, the entire building supported by the piles stoutly resists the large shear force. As a result, extraordinarily large interstory drift and shear force are produced in the first story where there exists a big gap of external force. We need to be aware that the remarkable building performance cannot be predicted by a base-fixed building response approach.

Likewise, the vertical distributions of the wood building are compared among the three kinds of soils in Fig. 7. Regardless of the kinds of soils, very large interstory drift and shear force were observed. In the liquefaction analysis of soils, because of the light flexible superstructure and the thin embedment (no embedment in

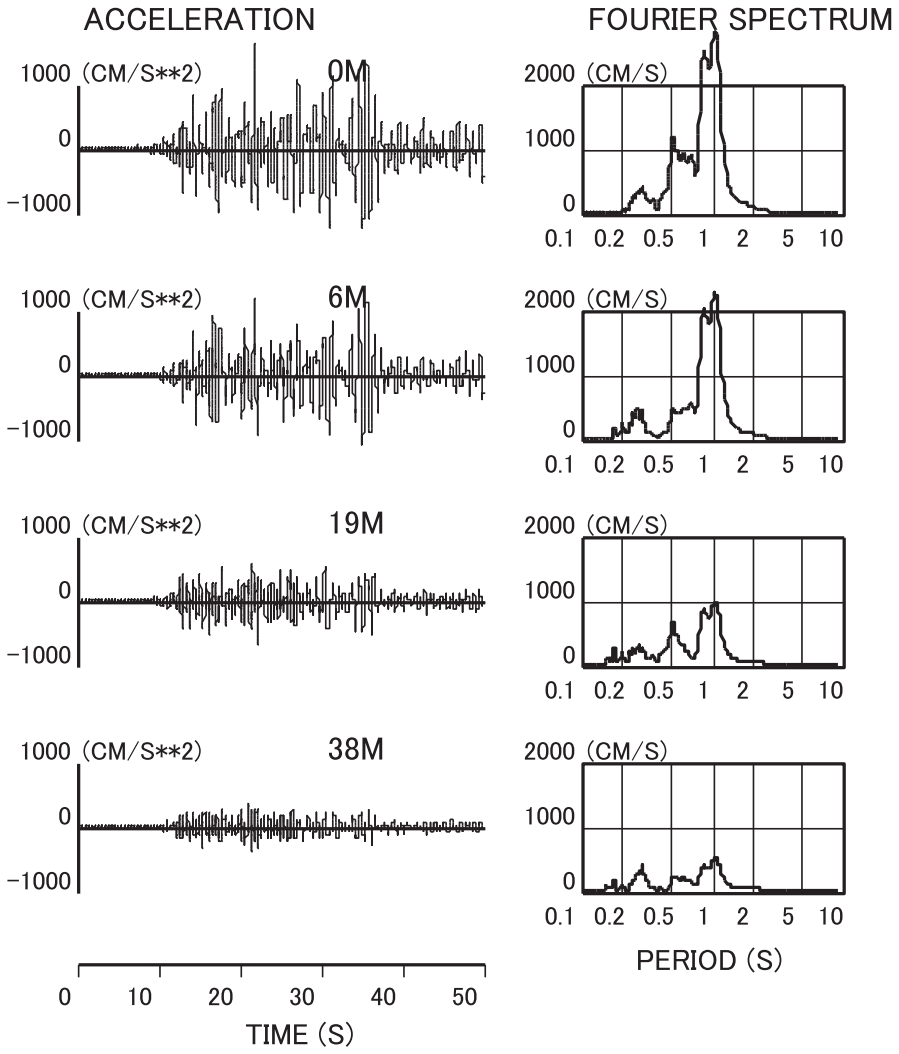

Fig. 5. FE liquefaction-simulated soil responses at four depths based on liquefaction-modified input wave field estimated at Echujima station for the 1923 Kanto earthquake

Table 3. Parameters Used for Superstructures and Foundations of the Two Buildings

Building	8 stories, RC	2 stories, wood
	Superstructure	
Height of each story (m)	3.0	2.7
Mass of each story (t)	509	5.6 (2)
		10.2 (1)
Stiffness of each story (kN/m)	1.20×10^6 (4-8)	706 (2)
	1.23×10^6 (3)	1,663 (1)
	1.27×10^6 (2)	
	1.66×10^6 (1)	
Yield shear strength of each story (kN)	4,988 (4–8)	16.1 (2)
	6,987 (3)	37.8 (1)
	9,290 (2)	
	11,976 (1)	
Fundamental period (s)	0.68	0.74
	Foundation	
Mass (t)	408	37
Embedment (m)	2.0	0.0
Length and width (m)	24 and 16	10 and 6

Note: Numerical values in parentheses are story numbers.

Table 4. Parameters Used for Concrete-Filled Steel Piles of the 8-Story RC Building

Building	8 stories, RC
Number	12
Length (m)	40.0
Radius (m)	0.50
Elastic modulus (kN/m^2)	1.47×10^7
Density (t/m^3)	2.4
Pure yield bending moment (kN m)[a]	1,600
Maximum yield bending moment (kN m)	2,600

[a]Pure yield bending moment = yield bending moment without axial force.

the model) of the foundation without piles, the entire building vibrated very severely on the 2-m nonliquefied soil layer that laid over the liquefied soil layers. Hence, extraordinarily large interstory drift and shear force were yielded in the two stories. Attention should be paid to the contrasting vibration characteristics of the two resonant buildings.

Table 6 summarizes the maximum response values at the head of a corner pile of the RC building calculated by the three types of

Table 5. Maximum Response Values of Superstructures of the Two Buildings Calculated by the Three Types of Analyses

	8 stories, RC			2 stories, wood		
Building analysis	Linear	Nonlinear	Liquefaction	Linear	Nonlinear	Liquefaction
Top-story acceleration (cm/s^2)	3,842	2,646	10,160	3,223	2,546	7,929
Top-story displacement (cm)	40.2	29.9	113.0	48.2	35.6	184.0
Maximum interstory drift through all stories (cm)	7.2	5.4	42.9	25.0	18.9	101.2
Ratio of the shear force to the yield strength of the first story (%)	795	641	11,623	1,031	756	4,448

Note: Top-story absolute accelerations include rocking; the top-story relative displacements with regard to foundation do not include rocking.

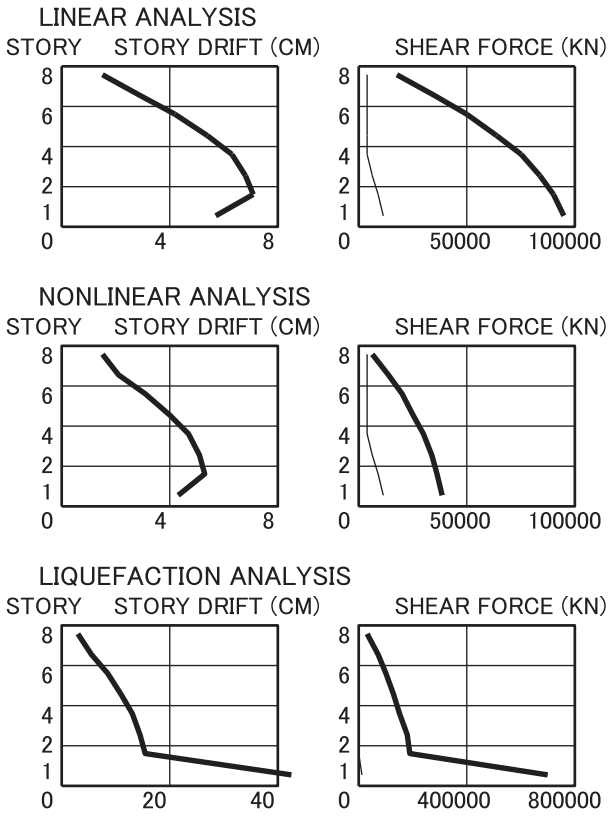

Fig. 6. Vertical distributions of maximum interstory drift and maximum shear force of the 8-story RC building calculated by the three types of analyses (thick lines); straight thin lines indicate yield strength

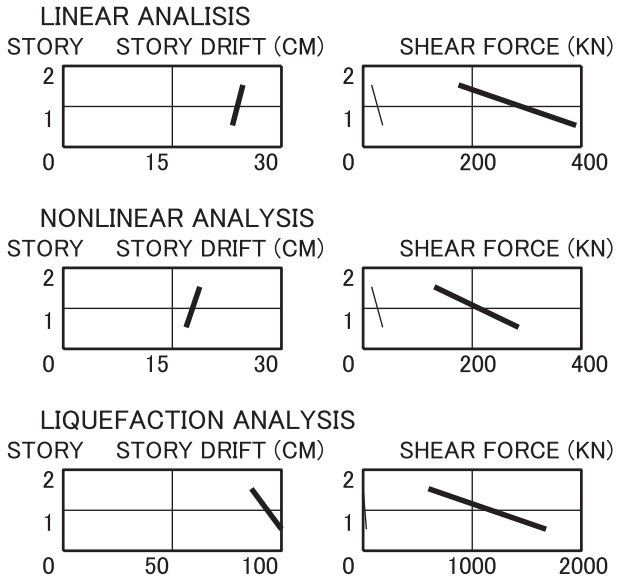

Fig. 7. Vertical distributions of maximum interstory drift and maximum shear force of the 2-story wood building calculated by the three types of analyses (thick lines); straight thin lines indicate yield strength

Table 6. Maximum Response Values at Head of Corner Pile of 8-story RC Building Calculated by the Three Types of Analyses

Analysis	Linear	Nonlinear	Liquefaction
Shear force (kN)	7,634	3,783	43,022
Axial force (kN)	31,850	14,700	73,108
Bending moment (kN m)	9,731	5,253	63,994

analyses. The bending moment at the pile head might be considerably overestimated because of the rigid connection between the pile and the foundation and also because of the linear behavior of the pile. In the linear analysis, the bending moment at the pile head goes beyond the maximum yield bending moment. The nonlinear behavior of the soil makes the bending moment considerably small. In the liquefaction analysis of soils, the bending moment becomes abnormally large. Besides, the bending moment of the pile became very large as well in the fully liquefied soils between 2 and 10 m depth (not shown here). Judging from the moment capacity, the pile head should sustain extremely severe damage.

Discussion and Conclusions

In this final section, Japanese RC building damage is interpreted based on the performance of the midrise RC building in the present study. The performance of the RC building is summarized as follows. First, the RC building responses evaluated in the cases of soils with linear and nonlinear behavior indicated damage of lower stories or piles. Second, liquefied soils greatly increased responses of the first story and the pile portions in liquefied soils. The partially increased responses were attributed to the highly decreased rigidity of liquefied soils and the resultant large increase in the amplitudes of surface waves. Third, in a previous study (Iida et al. 2015), the linear RC building responses evaluated in the case of elastic soils were basically similar to those calculated by a base-fixed building response analysis and by a conventional soil–building interaction analysis.

In large earthquakes in Japan, RC building damage has been concentrated on the first story of the building at a soft-soil site, along with occasional foundation damage. Specifically, neither midstory collapse nor top-story collapse has been observed, except for the 1995 Hyogoken-Nanbu earthquake ($M_J = 7.2$). This inland shallow earthquake produced very large (approximately 1,000 cm/s^2) ground motions in the epicentral regions, and caused heavy damage to various stories of the building and also to the pile foundation

(Earthquake Engineering Research Institute 1995). Many midstory collapses of RC buildings and steel reinforced concrete (SRC) buildings were noticeably observed. Japanese SRC buildings and the typical damage due to the 1995 event were described in a report by Azizinamini and Ghosh (1997). The damage pattern of the 1995 event was very different from those of other large events.

Numerous investigations have been performed to explain a variety of heavy damages caused by the 1995 Hyogoken-Nanbu earthquake. Some parts of these investigations extensively studied the dynamic performances of RC buildings and SRC buildings (Hayashi et al. 1999; Nagato and Kawase 2004). Among others, not a few studies attempted to interpret midstory building collapses, showing plausible response results (Kitamura et al. 1998; Nakamura and Yoshimura 2002). In such a situation, the SRC and the RC building responses (interstory drifts), provided by Hayashi et al. (1999) and by Nagato and Kawase (2004) respectively, are roughly similar to the RC building responses evaluated in the cases of soils with linear and nonlinear behavior in the present study, in spite of the different target earthquakes. Thus, it is considered that most damaged buildings suffered heavy structural damage because of severe vibration during the 1995 event.

In contrast, in large Japanese earthquakes, RC building damage has been concentrated on the first story. As far as the author knows, no general explanations for the first-story damage have been addressed up to now. In this context, the responses of the midrise RC building evaluated in the case of liquefied soils in the present study indicated that building damage took place in the first story. The building responses qualitatively explain the real typical damage pattern. Presumably, the building damage that occurred in the first story should be related to ground failure. Ground failure includes very strong nonlinear behavior of soils, liquefaction, and various landslides that were not taken into account in the present study. The building responses tell us that appropriate combined consideration of the foundation, the soils, and the ground motions is required to interpret the first-story damage.

In the liquefaction analysis of soils, the soil parameters have large uncertainties, and this issue should be further examined. For example, the effects of liquefaction on the building responses should be excessively overestimated because the assumption of full liquefaction is extreme. If the moderate degree of liquefaction were assumed, the effects of liquefaction would be decreased. Importantly, surface waves (Love waves) with extremely large increase in the amplitudes in liquefied soils make a large contribution to the building responses.

These explanations might not be applicable to RC building damage in other countries, mainly because building codes differ greatly from country to country. For instance, RC buildings in Mexico City are very flexible with extremely low stiffness in upper stories. Besides, long-period (approximately 2.0 s) ground motions are exceedingly dominant in Mexico City Basin (Iida 2013). Accordingly, RC building damage in Mexico City is considered to be very different from RC building damage in Japan. As an additional remark, unfortunately, no strong-motion accelerograms recorded during the 1923 Kanto earthquake exist. This lack of recordings causes large uncertainties in estimating strong-motion accelerograms for that event. Hence, the building performances obtained in the present study should be considerably overestimated because this study intends to avoid underestimation.

In this paper, 3D simplified nonlinear methods for examining the soil–building interaction for nonlinear behavior of soils based on an input seismic wave field were proposed. Interaction analyses of a midrise RC building and a wood building were performed in the cases of soils with linear, nonlinear, and liquefaction behavior in the reclaimed zone of Tokyo Bay for the 1923 Kanto earthquake. The main conclusions are as follows: (1) the interaction analyses provided reasonable evaluation of building performances; (2) in particular, building responses were excessively large after an extremely large increase in the amplitudes of surface waves in liquefied soils; and (3) the building responses provide significant hints for interpreting a typical damage pattern in which Japanese RC building damage is concentrated on the first story.

Acknowledgments

The majority of the accelerograms in this paper were provided as the data set of Strong Motion Array Observation No. 2 by the Association for Earthquake Disaster Prevention of Japan. Parts of the accelerograms of the Echujima station were provided by the Shimizu Corporation of Japan. Dr. Shunichi Fukumoto of the Tokyo Soil Research Corporation of Japan gave helpful advice on nonlinear and liquefaction behaviors of soils. Critical readings by two anonymous reviewers greatly improved the manuscript.

Notation

The following symbols are used in this paper:

$[C]$ = damping matrix;
$\{F\}$ = external force vector;
FSd = Fourier spectrum of a seismogram at a depth of d;
$FSRd1/d2$ = Fourier spectral ratio between two seismograms at depths of $d1$ and $d2$;
h = damping coefficient;
$[K]$ = stiffness matrix;
$[M]$ = mass matrix;
M_J = earthquake magnitude;
p = external displacement contributed by S waves;
q = external displacement contributed by surface waves;
t = time; and
$\{\chi\}$ = displacement vector associated with the system.

References

Azizinamini, A., and Ghosh, S. K. (1997). "Steel reinforced concrete structures in 1995 Hyogoken-Nanbu earthquake." *J. Struct. Eng.*, 10.1061/(ASCE)0733-9445(1997)123:8(986), 986–992.

Bielak, J., and Christiano, P. (1984). "On the effective seismic input for non-linear soil-structure interaction systems." *Earthquake Eng. Struct. Dyn.*, 12(1), 107–119.

Building Center of Japan. (2013). *The building standard law of Japan (enforcement order of building standard law, Chapter 3, Section 8)*, Tokyo.

Earthquake Engineering Research Institute. (1995). "The Hyogo-ken Nanbu earthquake, January 17, 1995." *Preliminary Reconnaissance Rep., 95–04*, Oakland, CA.

Hayashi, Y., Tamura, K., Mori, M., and Takahashi, I. (1999). "Simulation analyses of buildings damaged in the 1995 Kobe, Japan, earthquake considering soil-structure interaction." *Earthquake Eng. Struct. Dyn.*, 28(4), 371–391.

Iida, M. (1999). "3D analysis of S-wave propagation in soft deposits." *J. Geotech. Geoenviron. Eng.*, 10.1061/(ASCE)1090-0241(1999)125:9(727), 727–740.

Iida, M. (2006). "Three-dimensional linear and simplified nonlinear soil response methods based on an input wave field." *Int. J. Geomech.*, 10.1061/(ASCE)1532-3641(2006)6:5(342), 342–355.

Iida, M. (2013). "Three-dimensional finite-element method for soil-building interaction based on an input wave field." *Int. J. Geomech.*, 10.1061/(ASCE)GM.1943-5622.0000232, 430–440.

Iida, M., and Hatayama, K. (2007). "Effects of seawater of Tokyo Bay on short-period strong ground motions." *Bull. Seismol. Soc. Am.*, 97(4), 1324–1333.

Iida, M., Iiba, M., Kusunoki, K., Miyamoto, Y., and Isoda, H. (2015). "Seismic responses of two RC buildings and one wood building based on an input wave field." *Int. J. Geomech.*, 10.1061/(ASCE)GM.1943-5622.0000444, 04014093.

Iida, M., and Kawase, H. (2004). "A comprehensive interpretation of strong motions in the Mexican Volcanic Belt." *Bull. Seismol. Soc. Am.*, 94(2), 598–618.

Iida, M., Yamanaka, H., and Yamada, N. (2005). "Wavefield estimated by borehole recordings in the reclaimed zone of Tokyo Bay." *Bull. Seismol. Soc. Am.*, 95(3), 1101–1119.

Ishihara, T., and Miura, F. (1993). "Nonlinear seismic response analysis method for 3-D soil-structure interaction systems." *Proc. Japan Soc. Civ. Eng.*, 465(I-23), 145–154 (in Japanese).

Johnson, L. R., and Silva, W. (1981). "The effects of unconsolidated sediments upon the ground motion during local earthquakes." *Bull. Seismol. Soc. Am.*, 71(1), 127–142.

Kim, Y. S., and Roesset, J. M. (2004). "Effect of nonlinear soil behavior on inelastic seismic response of a structure." *Int. J. Geomech.*, 10.1061/(ASCE)1532-3641(2004)4:2(104), 104–114.

Kinoshita, S., Fujiwara, H., Mikoshiba, T., and Hoshino, T. (1992). "Secondary Love waves observed by a strong-motion array in the Tokyo lowlands, Japan." *J. Phys. Earth*, 40(1), 99–116.

Kitamura, H., Teramoto, T., Ukai, K., Murakami, K., Akiyama, H., and Wada, A. (1998). "Research of structural damage in the Hyogoken-Nanbu earthquake: Estimation of seismic energy input based on damage of structures." *J. Struct. Constr. Eng., Archit. Inst. Jpn.*, 503, 165–170 (in Japanese).

Koutsourelakis, S., Prevost, J. H., and Deodatis, G. (2002). "Risk assessment of an interacting structure-soil system due to liquefaction." *Earthquake Eng. Struct. Dyn.*, 31(4), 851–879.

Maheshwari, B. K., and Sarkar, R. (2011). "Seismic behavior of soil-pile-structure interaction in liquefiable soils: Parametric study." *Int. J. Geomech.*, 10.1061/(ASCE)GM.1943-5622.0000087, 335–347.

Nagato, K., and Kawase, H. (2004). "Damage evaluation models of reinforced concrete buildings based on the damage statistics and simulated strong motions during the 1995 Hyogo-ken Nanbu earthquake." *Earthquake Eng. Struct. Dyn.*, 33(6), 755–774.

Nakamura, T., and Yoshimura, M. (2002). "Earthquake response of concrete buildings suffering intermediate-story collapse during Hyogoken-Nanbu earthquake." *J. Struct Constr. Eng., Archit. Inst. Japan*, 556, 123–130 (in Japanese).